Characterizing global forest canopy cover distribution using spaceborne lidar

Characterizing global forest canopy cover distribution using spaceborne lidar

Hao Tang[a, *]

htang@umd.edu

John Armston[a]

Steven Hancock[b]

Suzanne Marselis[a]

Scott Goetz[c]

Ralph Dubayah[a]

[a]Department of Geographical Sciences, University of Maryland, College Park, MD, United States

[b]School of Geosciences, University of Edinburgh, United Kingdom

[c]School of Informatics, Computing, and Cyber Systems, Northern Arizona University, AZ, United States

*Corresponding author at: 1150 Lefrak Hall, University of Maryland, College Park, MD 20742, United States.

Edited by Jing M. Chen

Abstract

Detailed characterization of global forest dynamics requires accurate measurements of canopy cover beyond estimating the extent of forested area. Passive-optical remote sensing techniques, despite remarkable success in identifying global hotspots of forest cover loss, cannot fully satisfy observation requirements at the plot or canopy crown level. Critical issues including signal saturation and algorithm uncertainty impose limitations on capturing subtle canopy cover changes using standard products generated from satellite imagery, particularly over largely intact dense tropical forests. Spaceborne lidar remote sensing can fill this gap in contemporary Earth observation networks by providing direct measurements of 3-D canopy structure. Here we analyze global canopy cover distributions using observations from the Geoscience Laser Altimetry System (GLAS) onboard of NASA's Ice, Cloud, and land Elevation Satellite (ICESat-1). We found ICESat-based cover estimates were sensitive to canopy cover dynamics even over dense forests with cover exceeding 80% and were able to better characterize biome-level gradients and canopy cover distributions than the existing products derived from conventional optical remote sensing. At the footprint level, ICESat-1 produced almost no bias when compared with airborne estimates, and had RMSE values on the order of ~20% cover. Improved cover products based on lidar should allow comprehensive analysis of subtle forest structure changes at landscape scales, and provide unique information for biophysical stratification of forests and changes in vertical canopy structure. This is particularly true given the Global Ecosystem Dynamics Investigation (GEDI) lidar recently installed on the International Space Station, which will acquire higher resolution lidar data at greater sampling densities than has been available to date.

Keywords: Canopy ~~C~~cover; Forest structure; ICESat; Lidar; Tropical ~~F~~forests

~~1.~~1 I~~NTRODUCTION~~ntroduction

Canopy cover is an important biophysical variable widely used in global climatic, ecological, hydrologic and biodiversity studies (Bonan and Doney, 2018; Goetz et al., 2015; Lewis et al., 2015; Saatchi et al., 2011). Field measurements of canopy cover, together with other forest inventory data, are often used for analyzing long-term changing trends of forests and exploring their interactions with environmental change. However, high labor costs limit field-based sampling and thus can introduce bias and uncertainty over broad geographical extents (Malhi et al., 2006; Pan et al., 2011). Alternatively, field and inventory measurements may be coupled with satellite data to more efficiently generate estimates of canopy cover regionally and globally using a consistent spatio-temporal framework (e.g. Hansen et al., 2013). Indeed, satellite-based canopy cover monitoring has evolved remarkably over the past few

decades, from earlier work identifying deforestation hotspots (Skole and Tucker, 1993) to more recent efforts tracking annual global forest cover gain and loss at 30 m resolution (Achard et al., 2014; Hansen et al., 2013; Sexton et al., 2013; Townshend et al., 2012). These advances have increased our knowledge of global forest dynamics and its role in global climatic and environmental change (Bonan and Doney, 2018; Curtis et al., 2018; Watson et al., 2018).

The aforementioned maps of forest cover have primarily been used for detecting deforestation. However, a key limitation of these maps is that they typically have limited ability for differentiating subtle changes in canopy cover (e.g. <~10%) (Goetz et al., 2015; Hansen et al., 2008; Staver and Hansen, 2015). This is partially because these products were initially designed to estimate the total crown-covered area rather than smaller gap changes within otherwise intact forests. A typical algorithm that generates canopy cover from passive optical remote sensing data, such as Landsat imagery, first explores empirical relationships between spectral reflectance signals and reference data sets created from high-resolution imagery (e.g. Google Earth), and then applies these relationships over larger areas (Hansen et al., 2013). Data sets produced this way inherit the definition of *tree crown cover* used in the training process of high-resolution imagery, that is, "the vertical projection of the outermost perimeter of the natural spread of the foliage of plants" (Jennings et al., 1999). This definition is different from *canopy fractional cover*, which describes the percent of a fixed area covered by the vertical projection of canopy structural elements (e.g. numerically smaller by excluding openings in the crown) (Armston et al., 2009; Hansen et al., 2003; Rautiainen et al., 2005). As such, most imagery-based products are designed to have greater sensitivity to the presence of tree crowns (or their probability) than characterizing canopy fractional cover within crowns, which can be difficult to estimate even from ultra-high resolution imagery. Many other factors may contribute to the relatively large uncertainties that exist in canopy fractional cover estimates made from satellite imagery, including cloud and canopy shadows, decoupling woody and herbaceous cover, slope attenuation and signal saturation (Armston et al., 2009; Asner and Warner, 2003; Riano et al., 2003; Song and Woodcock, 2003). While the two canopy cover definitions share similarities and both can be used to map forest extent via thresholds, their impacts on ecological processes differ considerably. For example, small-scale gaps within intact forests missed by total crown cover are crucial for canopy radiation penetration, forest regeneration and tree species-diversity (Wright et al., 2010). The two therefore should not be used interchangeably although many studies do so or empirically scale one to the other due to the lack of a true canopy fractional cover product (Fisher et al., 2018; Yuan et al., 2014).

A second major limitation of canopy cover products derived from passive optical satellite imagery is their low sensitivity to high cover in densely forested areas. Whereas limited sensitivity may have minimal impact on delineating forest/non-forest extent, it is critical for characterizing canopy cover losses associated with other ecological processes in dense forests (e.g. tree mortality and demography). Dense canopies, mostly found across humid tropical regions, often have unique microenvironment conditions that differ seasonally and inter-annually from surrounding forests (Brando et al., 2010). Data from passive optical sensors often fail to provide reliable cover estimates over these dense canopy forests as they suffer signal saturation limiting direct observation of sub-canopy conditions (Huete et al., 2002). A simple but imperfect solution is to set a maximum detectable threshold above which all estimates are limited. For example, the MODIS Vegetation Continuous Fields (VCF) products (Hansen et al., 2003) set a global saturation threshold of 80%, and similar strategies apply to finer resolution sensors such as Landsat (Sexton et al., 2013; Townshend et al., 2012).

A third issue with prevailing satellite-based canopy cover products arises from the processing methods used. Hanan et al. (2014) reported discontinuities of tree cover estimates in current remote sensing products by comparing the MODIS VCF product to a pseudo-tree cover data derived from field measurements, arguing these discontinuities may be an artifact of the classification and regression tree (CART) processing algorithm used to derive the canopy cover products. This discontinuity, possibly due to binning bias (Gerard et al., 2017), raised concerns about the applicability of MODIS VCF, for example, in analyzing alternate stable states in tropical savannas and forests (Hirota et al., 2011; Staver et al., 2011). A follow-up technical response (Staver and Hansen, 2015) provided evidence of the unbiased estimates of the CART-generated tree cover by reanalyzing the real error distributions of the MODIS VCF data. Although this issue remains contested, these studies underscore the importance of having better calibrated and validated global cover products.

We argue that one way to address the issues that arise from the use of passive optical data is to employ more direct measures of 3D canopy structure, such as those derived from lidar. Lidar is a modern remote sensing technology that has already been widely used for deriving canopy cover products across various forest biomes (Armston et al., 2013; Goetz and Dubayah, 2011; Hopkinson and Chasmer, 2009; Korhonen et al., 2011; Lefsky et al., 2002; Morsdorf et al., 2006). Most of these studies use airborne lidar data, and are thus executed over relatively limited geographic extents. An attractive alternative is to generate global canopy cover products from spaceborne lidar, mirroring studies which have used such observations for mapping global canopy height and aboveground biomass (Baccini et al., 2012; Lefsky, 2010; Saatchi et al., 2011; Simard et al., 2011). The only spaceborne lidar whose data were suitable for global vegetation studies was the Geoscience Laser Altimeter System (GLAS) onboard NASA's Ice, Cloud, and land Elevation Satellite (ICESat-1), deployed between 2003 and 2009 (Abshire et al., 2005). A new ecosystem lidar recently launched in December 2018, the Global Ecosystem Dynamics Investigation (GEDI) Lidar (Dubayah et al., 2014), will include data products on canopy cover. It is thus of considerable interest to derive canopy cover from GLAS data, both by itself, and for comparison with GEDI products once they become available, to assess changes in cover over recent decades.

Here we report on global canopy cover distributions derived using ICESat-GLAS data, with a primary focus on humid tropical evergreen forests where current forest cover estimates have the greatest uncertainty. We assess the likelihood of robustly detecting high canopy cover (>80%) over these forests and independently assess performance of our cover estimates using airborne lidar measurements over dense tropical forests in Africa. We also compare footprint-level estimates with those from airborne waveform lidar as well as with global products derived from MODIS. Finally, we explore canopy cover distributions across major biomes and present an analysis of forest cover seasonal dynamics.

~~2.~~2 M~~ATERIALS~~aterials ~~AND~~and ~~METHODS~~methods

ICESat-GLAS recorded sample-based transects of canopy structure with a series of ~65 m footprints illuminated by a 1064 nm (near infrared) full-waveform lidar sensor (Abshire et al., 2005). The ICESat footprints have an along-track spacing of ~175 m and a maximum between-track distance of ~30 km at the Equator. Forest structural information, including canopy height and aboveground biomass, can be retrieved from ICESat data and its efficiency and accuracy have been thoroughly investigated in many studies and widely applied across major biomes of the world (Baccini et al., 2012; Los et al., 2012; Nelson et al., 2009; Saatchi et al., 2011; Tang et al., 2016). These applications increase our confidence in generating canopy fractional cover products at a global scale.

~~2.1.~~2.1 ICESat GLAS ~~P~~processing

We analyzed GLA14 lidar data sets from laser operation campaigns between 2003 and 2007 that cover three major seasonal periods: late February to March, late May to June, and October to November. We did not use laser campaigns after 2007 due to a well-documented degraded laser energy issue that impacted measurement consistency through time (NSIDC Distributed ICESat GLAS Laser Operations Periods: updated Dec. 2014). The data set included Gaussian fitting parameters of decomposed waveforms and other ancillary information such as acquisition time and geolocation. We further screened the footprint data set by applying predefined thresholds on cloud mask, topographic slope and signal saturation (Los et al., 2012). We then calculated the footprint-level canopy cover fraction as the ratio between vegetation return and the weighted total waveform energy. To account for the difference between canopy and ground apparent reflectance, we used a global average reflectance ratio of 1.5 for simplicity, although this value may vary in space and time from about 1.0 to 2.0 at the footprint level ~~in space and time~~ (Harding et al., 2001; Tang et al., 2012). This variation has a small effect on canopy cover estimates at the high end but may have a relatively greater impact at the lower range (Harding et al., 2001). In addition, we applied a recursive analysis to refine initial canopy cover estimates by mitigating slope effects and rejecting possible outliers based on search of maximum potential leaf area index (Tang et al., 2014). More detailed information can be found in the ~~s~~Supplementa~~l~~ry material.

~~2.2.~~2.2 Airborne waveform lidar processing

The accuracy of ICESat-GLAS canopy cover at the high cover range was examined with a comparison to airborne lidar measurements over a dense tropical forest in Africa. The airborne canopy cover reference was derived from flights in Gabon using NASA's Land Vegetation and Ice Sensor (LVIS) (Blair et al., 1999) as part of a joint NASA-ESA-DLR (European Space Agency-German Aerospace Center) AfriSAR campaign in February and March 2016 (Fatoyinbo et al., 2017). During the campaign, LVIS completed a ~170 km acquisition of the ICESat-1 ground path, providing an opportunity to assess the ICESat estimates. Canopy cover, along with other ecological metrics, were generated for LVIS footprints (~25 m) over dense forests using the methodology of Tang et al. (2012). In comparison to earlier data collections, the LVIS instrument used for the Gabon acquisitions was redesigned and upgraded, with greater signal to noise properties that are sensitive to detecting canopy fractional cover exceeding 99%, which makes it more suitable for assessing the performance of ICESat GLAS data over extremely dense forests. We made footprint-level comparisons between ICESat and LVIS acquisitions, as well as landscape-level comparisons using aggregated observations along the 4-km LVIS flight swath. The comparisons were conducted following visual inspection of Landsat imagery to ensure that no areas with deforestation or forest degradation were included. Shrublands and savannas areas were not included in the comparisons to avoid areas where changes ~~was~~ were more likely to occur over the ~10 year time period we examined. We then applied the Anderson-Darling (A-D) tests to compare the distributions of LVIS and ICESat forested footprints (cover >~10% and height >~5 m). We chose the A-D test rather than the Kolmogorov-Smirnov test because the latter is less sensitive to data at the tails of a distribution, which is the focus of our analysis.

In addition to the Gabon site, we included LVIS data from previous acquisitions to further assess the performance of ICESat at the footprint level in a range of different forest ecosystems. These included a wide gradient of canopy fractional cover in North and Central America, from the White River National Wildlife Refuge in Arkansas (2006), Sierra National Forest in California (2008), Baltimore–Washington corridor in Maryland (2003), forests north of Orono, Maine (2003), and tropical rainforests at the La Selva Biological Station, Costa Rica (2005) (Tang et al., 2012; Tang et al., 2016). We did not combine these sites with the Gabon data because of their large temporal difference and the use of an upgraded LVIS instrument in Gabon.

~~2.3.~~2.3 Ancillary data

We extracted ancillary information to ICESat footprints from conventional optical remote sensing products to facilitate its performance assessment at global scale and by different biomes. The ancillary information included the 250 m MODIS VCF product (MOD44B) (DiMiceli et al., 2011) and the 500 m MODIS land cover type product (MCD12Q1) (Friedl et al., 2010). We did not consider interannual variability given the short observation period of ICESat-1. Rather we calculated the average estimate of the annual VCF product and the majority type of the annual IGBP land cover classification between 2003 and 2007. We also extracted vegetation phenology information from MODIS land cover dynamics product (MCD12Q2), and identified the start and end of growing season as the median of annual increase and minimum of Enhanced Vegetation Index (EVI)-based greenness. We ignored phenological dynamics over evergreen forests (both needleleaf and broadleaf) due to large product uncertainty of MCD12Q2 and complexity of seasonal cycles, particularly over the tropics. Based on the above information and the forest definition of FAO, we classified the ICESat footprints into two categories: 1) vegetated footprints, including all ICESat footprints falling over forest, shrubland and savanna according to MODIS land cover type, and 2) forested footprints with total canopy fractional cover >~10% and canopy height exceeding 5 m (note this is a subset of the first category).

We then compared ICESat-derived canopy cover with MODIS VCF at both footprint and biome level over all vegetated areas globally. We performed an Anderson-Darling (A-D) test to examine the possible difference between the two canopy cover distributions. We estimated both the mean and probability distribution of ICESat canopy cover at 0.5° grid cells by aggregating leaf-on forested footprints. In particular, we assessed the chance of having very high canopy cover at the footprint level across the pan-tropical region (70%~90% and exceeding 90% respectively). Cells with fewer than 25 ICESat footprints were masked out in an attempt to minimize possible sampling errors in the aggregation process. The biome level canopy cover distributions were generated by pooling the vegetated footprints into six predefined land cover types (i.e. evergreen needleleaf forest, evergreen broadleaf forest, deciduous needleleaf forest, deciduous broadleaf forest, mixed forest, as well as shrubland and savanna).

We additionally investigated the seasonal dynamics of canopy cover across the tropics at 1° cells. Following Tang and Dubayah (2017), we calculated the mean differences among the vegetated footprints from the three ICESat seasonal periods, and then undertook a sensitivity analysis of the estimated change accounting for total shot number within each pixel and footprint-level accuracy of ICESat estimates. Here we applied a global average 10% measurement error, a value consistent with previous lidar studies (typically ranging from about 5% to 15% in comparison to field estimates, with smaller error for closed canopy) (Armston et al., 2013; Hopkinson and Chasmer, 2009; Korhonen et al., 2011; Morsdorf et al., 2006).

~~3.~~3 R~~ESULTS~~esults

In this section we present comparisons of ICESat, airborne lidar and MODIS cover estimates. These comparisons include analyses of the spatial patterns of ICESat-based canopy fractional cover regionally and at different biome levels.

~~3.1.~~3.1 ICESat vs. LVIS

Over the AfriSAR LVIS swath there were a total of 460,499 LVIS and 912 ICESat forested footprints which were used for statistical analyses (Fig. 1). The majority of LVIS and ICESat footprints in Gabon had a canopy cover ~~greater than~~ ≥85% with a peak around 95%~~ in Gabon~~. Although the ICESat data showed a relatively lower peak than LVIS cover estimates, the A-D test could not detect a statistically significant difference (p-value = 0.52). Their agreement at the footprint level was understandably low given a ~10 yr difference ($r^2 = 0.27$, bias = ~~-~~5.46, RMSE = 21.6%). Footprint-level comparison in North and Central America had better agreement, with an $r^2 = 0.57$, bias = ~~-~~2.05, RMSE = 16.87% (Fig. 2). In tropical rainforest sites, the comparison at La Selva produced an $r^2 = 0.45$, bias = 2.57, RMSE = 19.24%, slightly better than that in Gabon.

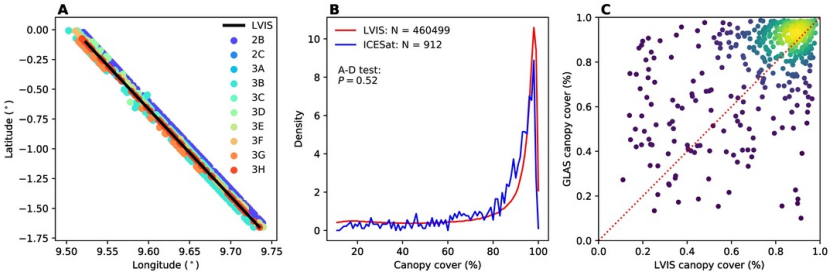

Fig. 1 Comparison between ICESat GLAS and airborne LVIS derived canopy cover in an African tropical rainforest (Rabi, Gabon). Panel A presents the geographical extent of the LVIS flight line (4-km swath) and corresponding ICESat GLAS footprints colored by laser campaigns from 2003 to 2007 (note different scales in latitude and longitude). Panel B shows canopy cover distributions aggregated from forested ICESat and LVIS footprints. The Anderson-Darling test cannot reject the null hypothesis that there is no difference between the two distributions. Panel C shows the footprint-level comparison result between ICESat and averaged LVIS estimates ($r^2 = 0.27$, bias = ~~-~~5.46, RMSE = 21.6%). Each point represents a footprint-level comparison case with the bright-yellow color indicating a high kernel density in the plot. (For interpretation of the references to color in this figure legend, the reader is referred to the web version of this article.)

alt-text: Fig. 1

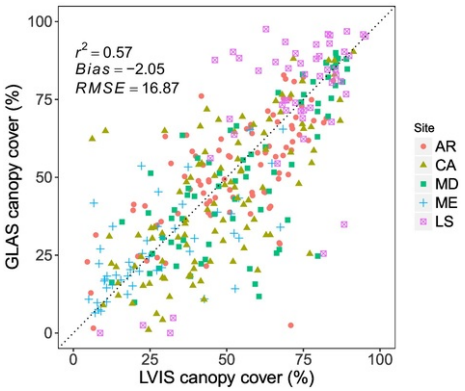

Fig. 2 A comparison between ICESat canopy cover and those derived from airborne LVIS campaigns between 2003 and 2008. Each data point represents a comparison at individual ICESat footprint, and different color-shape combinations indicate different forest types surveyed by the LVIS instrument (AR: 2006 White River National Wildlife Refuge in Arkansas; CA: 2008 Sierra National Forest in California; MD: 2003 Baltimore–Washington corridor in Maryland; ME: 2003 Maine forests to the north of Orono, Maine; LS: 2005 La Selva Biological Station, Costa Rica).

alt-text: Fig. 2

~~3.2.~~3.2 ICESat vs. MODIS VCF

At the global scale, canopy cover estimates from ICESat and MODIS VCF (Fig. 3) showed only moderate agreement ($r^2 = 0.30$, bias = ~~-~~0.88, RMSE = 26.2%). While the two data sets agreed on a bimodal pattern of canopy cover and showed almost no bias, only a small percentage of data points were distributed near 1:1 line between 25% and 75% canopy cover. There were discrete clusters in the VCF product relative to the ICESat cover estimates, with almost no VCF estimate ~~greater than~~ ≥80% canopy cover. The A-D test confirmed a significant difference between the two distributions (p-value <0.001). Their difference was more evident when assessed over different land cover types (Fig. 4), with substantial bias (>15%) and minimal correlation over evergreen needleleaf forest or mixed forest. There also appeared to be discrete clusters of tree cover in the VCF products in comparison to ICESat (e.g. two horizontally oriented clusters in Mixed Forest of Fig. 4).

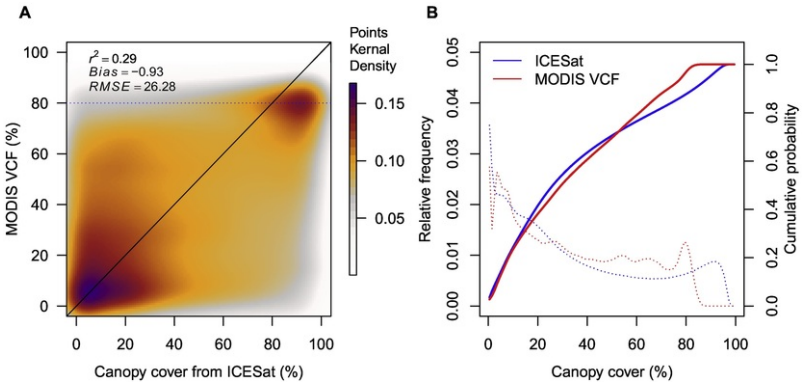

Fig. 3 Global comparison between MODIS VCF and ICESat canopy cover at footprint level (Panel A). In Panel B, dotted lines represent the probability distributions of ICESat canopy cover (blue) and MODIS VCF (red) over global vegetated areas, and solid lines are the correspondin cumulative distribution functions. (For interpretation of the references to color in this figure legend, the reader is referred to the web version of this article.)

alt-text: Fig. 3

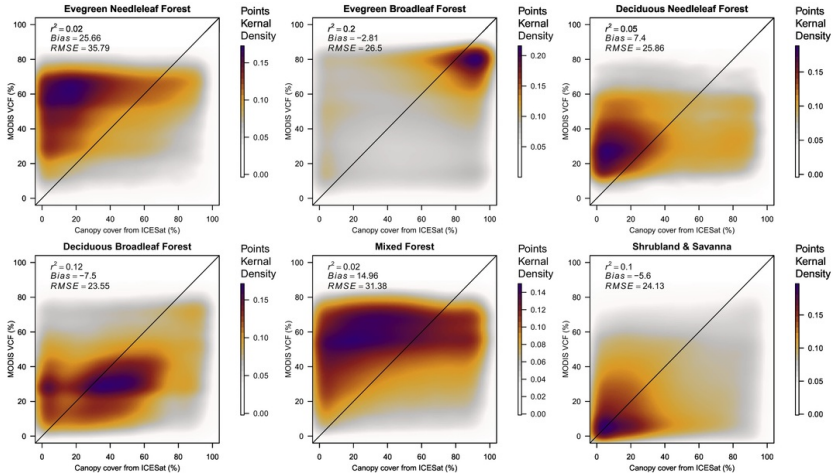

Fig. 4 Pixelwise comparison between MODIS VCF and ICESat canopy cover by land cover type.

alt-text: Fig. 4

We did not find any discontinuity in the ICESat canopy cover product along gradients grouped by land cover types (Fig. 5). We found canopy cover of both evergreen and deciduous needleleaf forests appeared as a Weibull distribution, with the peak (at about 10~~–~~15%) skewed ~~towards~~toward the lower end and a small percentage exceeding 80%. The spike at 0~~–~~2% range was probably caused by the non-random sampling pattern of ICESat and inaccurate classification of MODIS land cover type. Shrublands and savannas had a similar pattern as needleleaf forests, with slightly higher density below 30%.

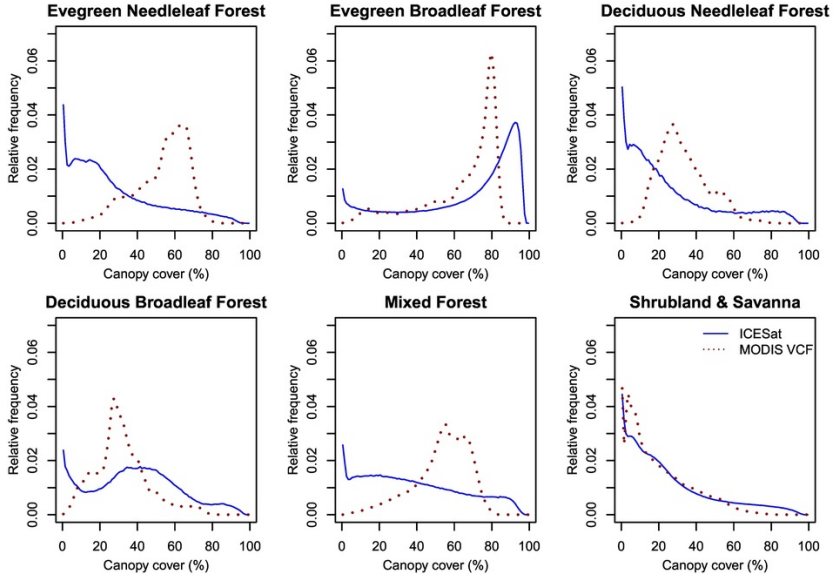

Fig. 5 Distributions of ICESat canopy cover (blue-~~solid~~solid) and MODIS VCF (red-dash) across different land cover types. These include all vegetated ICESat footprints (see definitions in Methods section 2.3). (For interpretation of the references to color in this figure legend, the reader is referred to the web version of this article.)

alt-text: Fig. 5

In contrast, broadleaf forests presented more complex patterns. While evergreen broadleaf forests showed a typical bimodal shape with the majority of footprints exceeding 70% canopy cover, deciduous broadleaf forests

displayed a trimodal distribution — two major peaks centered close to 0% and around 40% as well as a minor one at about 90%. Mixed forests, unlike any other types, showed a more even distribution across the entire spectrum aside from a spike below 2% and a small dip above 95%. The corresponding MODIS VCF estimates showed a continuous canopy cover distribution as well (only below 80%), but consistently with a unimodal shape by forest type. The peaks were centered around 5% for shrubland and savanna, 30% in deciduous broadleaf forest and needleleaf forest, 60% in evergreen needleleaf forest and mixed forest, and 80% in evergreen broadleaf forest. ICESat and MODIS agreed best at two extremes of canopy cover distribution, i.e. evergreen broadleaf forest and shrubland – savanna. However, ICESat produced much smaller canopy cover estimates in evergreen needleleaf forest and, unlike MODIS VCF, showed no major peak in mixed forest.

~~3.3.~~3.3 Spatial patterns of ICESat GLAS canopy cover

The ICESat GLAS canopy cover map over global forested areas (Fig. 6) revealed a distinct gradient across latitude bands, consistent with the global distribution of forested biomes (e.g. from dense humid tropical forest to sparse boreal evergreen and deciduous needleleaf forest). Areas with canopy cover ~~greater than~~ ≥80% predominantly occupied tropical forests in the Amazon basin, the Congo basin and the Malay Archipelago. Forested areas over the adjacent tropical savannas and shrublands tended to have a much lower canopy cover with estimates ranging from about 15% to 40%. Most temperate forests also showed high average values, albeit less than tropical forests (from about 50% to 80%). The cover values gradually decreased toward the polar regions, with most boreal forests over 50° N across North America and Eurasia having canopy cover values around 30%.

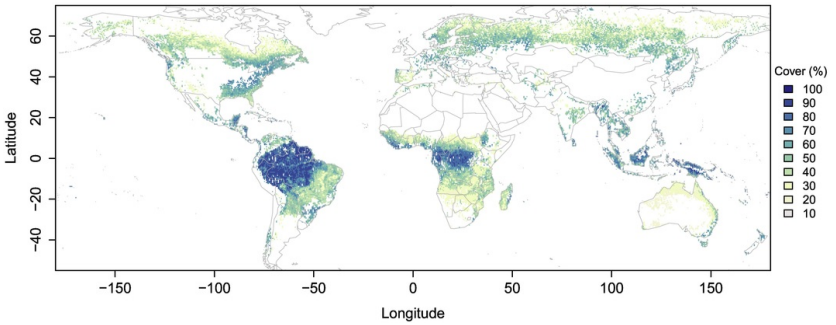

Fig. 6 A global 0.5° canopy cover map averaged from leaf-on forested ICESat GLAS footprints. Note these are only forested footprints with canopy cover >10% and height >5 m. Cells with 25 footprints or less were excluded from the analysis.

alt-text: Fig. 6

The aggregated ICESat GLAS data sets also characterized regional variations of canopy cover, particularly over high-density forests of the tropics (~~Fig. 7~~Figs. 7 and 8). Our results showed that the probability of having extremely dense canopy cover varied considerably across these regions. Amazonia had the greatest frequency of extremely high (e.g. >90%) canopy cover in the evergreen broadleaf forest class (Fig. 7D), particularly when compared to Tropical Africa and Southeast Asia. About 70% of forested ICESat footprints in the evergreen broadleaf forests of tropical America exceeded 80% canopy cover with about 60% exceeding this threshold in tropical Africa and ~~less than~~ ≤40% in Asia (~~Fig. 7~~8). Most forests and savanna areas outside the Amazon and Congo basins had much smaller probabilities of having extremely dense canopies (typically <10%). Areas having canopy cover between 30% and 50% included the Chaco of northwestern Paraguay, the Atlantic Forest of Brazil, and the dry forests of Angola, Zambia and central Madagascar (~~Figs. 7A, 8~~Fig. 7).

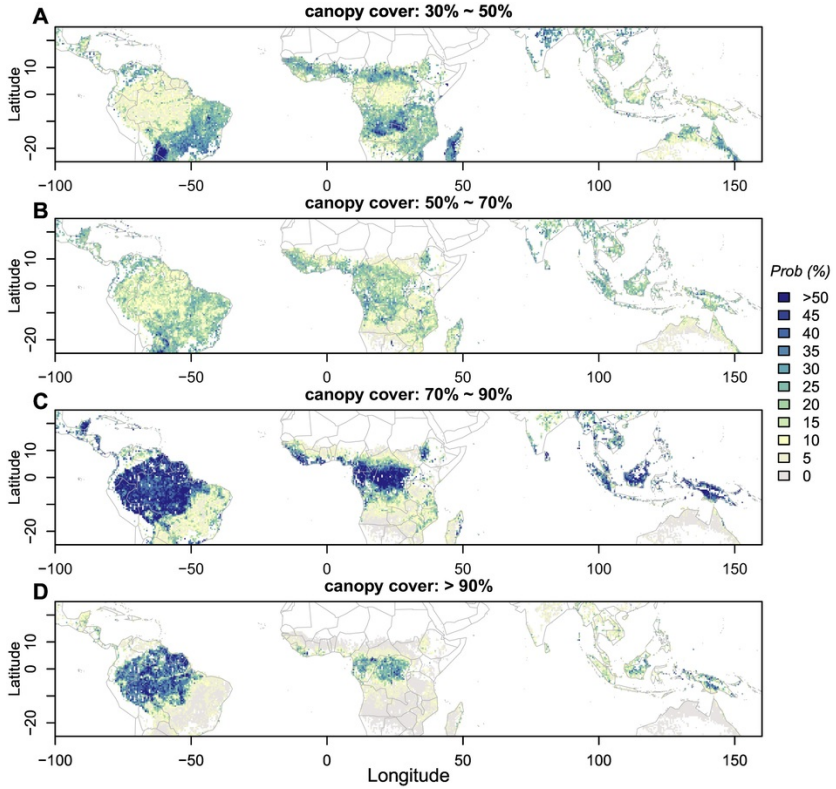

Fig. 7 The probability of a forested patch (~0.3 ha; a single ICESat footprint) having canopy cover between four predefined intervals based on the same data set used in Fig. 6. The total probability of these data sets are less than or equal to one.

alt-text: Fig. 7

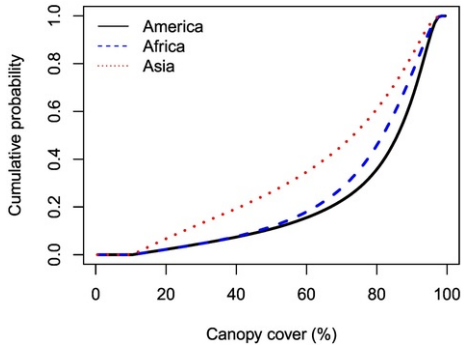

Fig. 8 Cumulative probability distributions of canopy cover of tropical evergreen broadleaf forests over three continents (Central and South America, Central Africa, and Asia-Pacific). The empirical distributions were generated from corresponding forested ICESat footprints (Fig. 7)

alt-text: Fig. 8

The ICESat canopy cover maps also captured seasonal changes in a similar way to conventional remote sensing (e.g. MODIS) (Fig. 9 and Supplementary Material). ICESat and MODIS-based EVI metrics had a very good agreement over tropical deciduous forest, woodland and savannas typically experiencing a single and strong seasonal cycle (e.g. monsoon). This seasonality was most evident in Eastern Miombo woodlands and East Sudanian savanna in Africa, Central Indochina dry forest in Southeast Asia and as well as Brazilian Atlantic dry forest. The seasonal pattern was also discernible in northern Australia during the southern hemisphere autumn-winter-spring cycle. However,

the two satellite data sets (MODIS and ICESat) did not generally agree over wet and moist tropical rainforests. There were even opposite patterns observed, for example, during the wet-dry transition period (March to June) in the southern Amazon forests: MODIS EVI indicating a decreasing trend but ICESat showing a distinct increasing one. These disagreements were not only due to the limited temporal sampling of ICESat but also caused by large uncertainties from MODIS data used to infer seasonality (e.g. BRDF corrections; see Supplementary Materials for more details).

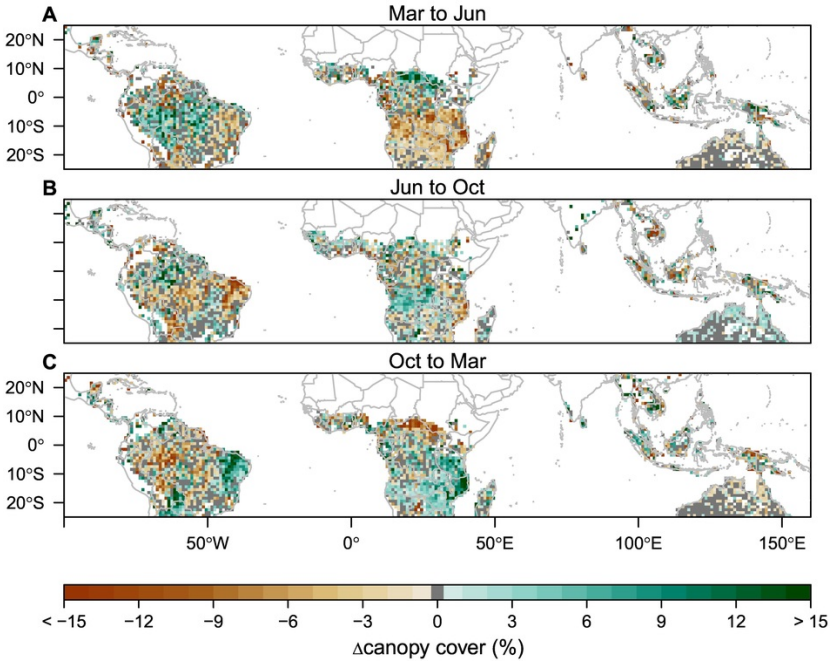

Fig. 9 Seasonal changes of canopy cover across tropical regions at 1° grid cells. Each cell represents the mean canopy cover change for 2003–2007 ICESat data aggregated in March, June and October (Gray pixels are areas with mean change less than the estimated error threshold). These temporal changes agree well with MODIS and knowledge of tropical deciduous forest, woodland and savanna ecosystems but show different patterns over wetter areas (e.g. Amazon rainforests).

alt-text: Fig. 9

4.4 DISCUSSIONiscussion

The overarching goal of our study was to explore global canopy cover distributions over forested areas using spaceborne lidar data. Our analysis thus differs from “area-focused” studies using passive optical sensors to map the geographical extent of forest cover and detect its temporal change (e.g. deforestation) (Achard et al., 2014; Hansen et al., 2013, 2008; Sexton et al., 2016). Our ICESat-based estimates instead provide the continuous canopy fractional cover in intact or degraded forests and those having recovered from disturbance events, a quality- or density-driven subject that remains poorly characterized due to insufficient precision of prevailing cover products over dense forests.

Lidar-based products can provide more direct and accurate estimates of canopy gap fraction and cover even in dense tropical forests. Following examples implemented at regional and landscape scales (Hopkinson and Chasmer, 2009; Morsdorf et al., 2006; Tang and Dubayah, 2017; Tang et al., 2012), our results provide further support that satellite observations capture the patterns and temporal variability of canopy cover, but for the first time at the global scale using spaceborne lidar, albeit at a coarser spatial resolution. Comparison with airborne lidar data collected over the entire spectrum of canopy cover increase our confidence in mapping forest cover with ICESat, even when cover values exceed 80% (Figs. 1 and 2). Despite relatively large footprint-level uncertainty (15–20% RMSE), the estimates of canopy cover convey a substantial reduction of uncertainty at the landscape level with increased sampling density. Note we did not focus on the repeatability at the footprint level because it is impractical given the orbit pattern of the spacecraft, which was designed to increase the spatial distribution of sampling at low and mid latitudes. Instead, the ICESat-based product was used for estimating the expected value of landscape-level ecological attributes and their dynamics in response to regional changes.

The strength of the ICESat GLAS canopy cover products lies in their direct estimates of canopy fractional cover. Our approach requires neither extensive field calibration nor complex model construction and sampling

stratification, both of which were required in the process of passive optical remote sensing imagery (e.g. MODIS and Landsat). Instead, the waveform measurements directly capture the profile of radiation attenuation within the canopy, and thus span the entire physical range of canopy cover in the vertical dimension. As a result, we do not observe any discontinuity in canopy cover distribution (Figs. 2, 3 and 4), a critique of a prevailing cover product from MODIS VCF (Hanan et al., 2014; Yuan et al., 2014).

Comparisons between MODIS VCF products and our ICESat GLAS canopy cover maps show a general agreement at the global scale, and confirm the low overall bias (<1%) of VCF products (Staver and Hansen, 2015). However, we find that the MODIS VCF may be a less than ideal reference at the biome level. For example, MODIS VCF product saturates at high canopy cover (>80%, most pronounced in evergreen broadleaf forests) (Fig. 2). There also appear to be discrete clusters in VCF compared with ICESat GLAS cover, particularly over mixed forests (Fig. 4), which is probably caused by the nature of the VCF training data, i.e. “a discrete classification of the Landsat data into 4 classes of relative percent tree cover (0, 25, 50, 80+)” (User Guide for MODIS VCF; DiMiceli et al., 2011). In addition, MODIS VCF shows a relative overestimation toward the ICESat cover product in needleleaf forests (Fig. 3) probably caused by different canopy cover definitions (Tang et al., 2019): VCF and similar satellite imagery primarily aim at estimating the mean crown cover while ICESat estimates the canopy fractional cover whose value is always smaller than crown cover. This means a decrease in MODIS VCF time-series may be better interpreted as loss of many individual crowns, such as those associated with forest clearing, rather than subtle changes in canopy cover often associated with small-scale natural disturbances or forest degradation. Even relatively finer resolution imagery such as Landsat may not be able to meet observation requirements for monitoring relatively small changes caused by physiological or phenological factors over dense intact forests (Goetz et al., 2015; Lewis et al., 2009). By contrast, ICESat GLAS-based estimates can better track these subtle changes, such as seasonal cycles of cover change in moist rainforests (Fig. 7). Seasonal changes, for instance, generally agree with the high-temporal dynamics of in situ observations acquired from ground-based lidar in the central Amazon (Smith et al., 2019). Yet the low temporal resolution of our ICESat GLAS gridded cover product makes it less than ideal for operational phenology applications, and can have substantial uncertainties in some of the dense tropical forests that experience more than one dry/wet seasonal cycle.

Our results have implications for future ecosystem monitoring and can help address issues associated with insufficient measurement precision from conventional passive optical remote sensing. For example, our results support the hypothesis of alternative stable states of tropical savanna-forest (Hirota et al., 2011; Staver et al., 2011), as the ICESat GLAS canopy cover estimates revealed contrasting patterns between evergreen broadleaf forests and shrubland-savanna (clustered at two extremes with sparse intermediate values) (Figs. 3 and ~~Fig.~~ 5). The cover plus height information, for example, can help identify the extent of forest in dryland biomes (Bastin et al., 2017). Over dense humid tropical forests, ICESat GLAS canopy cover estimates captured not only mean canopy cover distributions, but also variations at the extremes across large environmental gradients and seasonal cycles (Figs. 5, 6 and 7). Our findings suggest spaceborne lidar, when combined with ancillary information, can improve our capability of detecting canopy-scale changes caused by factors other than forest clearing (e.g. drought-driven tree mortality) over targeted ecoregions (Lewis et al., 2009; Phillips et al., 2009). There were more complex patterns of ICESat cover estimates in the temperate regions (Figs. 3 and ~~Fig.~~ 5), such as a trimodal frequency distribution over deciduous broadleaf forest areas, but a more even distribution of canopy cover across mixed forests. These results suggest there may be additional drivers of cover change within certain land cover types not captured in the MODIS VCF data (Fig. 5), such as different responses to regional climate conditions or human modification of forests.

Despites these advantages of mapping forest cover over broad geographical extents using satellite lidar data, limitations remain for characterizing vegetation structure more generally. The primary limitations arise from limited sampling densities in both the spatial and temporal domain (e.g. in the case of ICESat-1, wide cross-track distances and ~3-month revisit frequencies). It is also difficult to detect canopy changes at any given location given ICESat-1 did not acquire exact repeating orbits. Rather, ICESat footprints can be viewed as a pseudo-observation network with millions of plot-level observations, requiring spatial aggregation in order to describe forest structural changes. Our intent here was to keep the footprint-level observations at their native resolution and precision. Thus we did not use empirical models or satellite imagery to interpolate these estimates across space but instead performed spatial aggregation at 0.5° and change analysis at 1°, resolutions much coarser than many remote sensing imaging instruments (such as Landsat and Sentinel sensors). Nonetheless, gridded observations such as those we provide have utility for global scale earth system models as many of them are implemented at similar resolutions (Bonan and Doney, 2018). Moreover, we envision most of ICESat-1’s limitations will be resolved by NASA’s spaceborne vegetation lidar mission, the Global Ecosystem Dynamics Investigation (GEDI) (Dubayah et al., 2014). GEDI was successfully launched to the International Space Station (ISS) in December 2018, and began its science data collection on March 25, 2019. GEDI Lidar is expected to collect 10 billion cloud-free full waveform measurements similar to those provided by ICESat GLAS, but at much higher spatial resolution (25 m footprint) and sampling densities (60 m along-track and 600 m across-track). GEDI will acquire data over almost all temperate and tropical forests (about ±51.6° latitude), and both footprint level and gridded data products (at 1 km resolution) will be produced by the end of its nominal 2-year mission life, including leaf area index, foliage height diversity indices and canopy cover estimates. These products have the potential to provide a new baseline of global forest cover and, when combined with wall-to-wall data from passive optical and synthetic aperture radar instruments, should catalyze our ability to characterize the dynamics of forest cover changes at unprecedented accuracy.

~~5.~~5 C~~ONCLUSION~~onclusion

Characterizing canopy structure over extremely dense forests remains a challenge over humid tropical forests, where rapid canopy cover changes can take place at both landscape and more local scales, such as canopy gaps from selective logging operations or seasonal changes. Lidar remote sensing can fill the gap in contemporary satellite observation networks by providing more precise estimates of canopy structure changes. Our analyses with ICESat

data demonstrate the capacity of spaceborne lidar to directly measure canopy cover with no significant saturation issues. At the footprint level ICESat-1 cover estimates contain minimal bias when compared with airborne lidar cover estimates. At the regional scale ICESat GLAS canopy cover estimates characterize the spatial distribution and probabilities of extremely dense canopies, a pattern that is indiscernible when using passive optical sensors but critical for assessing subtle cover and structure changes caused by factors like canopy seasonality. Our results increase confidence in generating similar products from the GEDI Lidar mission, but at much higher spatial and temporal resolutions. These lidar-based data products complement existing satellite image products, and should significantly advance our ability to characterize dynamics of canopy structure through time. They will also enable a deeper understanding of global forest ecology and biodiversity.

~~ACKNOWLEDGEMENTS~~Acknowledgements

This study is funded by NASA's New Investigator Program (80NSSC18K0708), Global Ecosystem Dynamics Investigation (GEDI) mission (NNL15AA03C), and Applied Sciences Program (NNX17AG51G). The airborne lidar data is supported by NASA-ESA-DLR's AfriSAR campaign (NNX16AP74G). We also thank technical help and data support from Kim Calders, Temilola Fatoyinbo and Michelle Hofton.

~~Appendix A.~~Appendix A. Supplementary data

Supplementary data to this article can be found online at https://doi.org/10.1016/j.rse.2019.111262.

~~REFERENCES~~References

Abshire J.B., Sun X., Riris H., Sirota J.M., McGarry J.F., Palm S., Yi D. and Liiva P., Geoscience Laser Altimeter System (GLAS) on the ICESat Mission: ~~O~~on-orbit measurement performance, *Geophys. Res. Lett.* **32**, 2005, https://doi.org/10.1029/2005GL024028.

Achard F., Beuchle R., Mayaux P., Stibig H.-J., Bodart C., Brink A., Carboni S., Desclée B., Donnay F., Eva H.D., Lupi A., Raši R., Seliger R. and Simonetti D., Determination of tropical deforestation rates and related carbon losses from 1990 to 2010, *Glob. Chang. Biol.* **20**, 2014, 2540–2554, https://doi.org/10.1111/gcb.12605.

Armston J.D., Denham R.J., Danaher T.J., Scarth P.F. and Moffiet T.N., Prediction and validation of foliage projective cover from Landsat-5 TM and Landsat-7 ETM+ imagery, ~~*J. Appl. Remote Sens*~~*J. Appl. Remote. Sens.* **3**, 2009, 1–28 https://doi.org/10.1117/1.3216031.

Armston J., Disney M., Lewis P., Scarth P., Phinn S., Lucas R., Bunting P. and Goodwin N., Direct retrieval of canopy gap probability using airborne waveform lidar, *Remote Sens. Environ.* **134**, 2013, 24–38, https://doi.org/10.1016/j.rse.2013.02.021.

Asner G.P. and Warner A.S., Canopy shadow in IKONOS satellite observations of tropical forests and savannas, ~~*Remote Sens. Environ*~~*Remote Sens. Environ.* **87**, 2003, 521–533, https://doi.org/10.1016/j.rse.2003.08.006.

Baccini A., Goetz S.J., Walker W.S., Laporte N.T., Sun M., Sulla-Menashe D., Hackler J., Beck P.S.A., Dubayah R., Friedl M.A., Samanta S. and Houghton R.A., Estimated carbon dioxide emissions from tropical deforestation improved by carbon-density maps, *Nat. Clim. Chang.* 2012, https://doi.org/10.1038/nclimate1354.

Bastin J.-F., Berrahmouni N., Grainger A., Maniatis D., Mollicone D., Moore R., Patriarca C., Picard N., Sparrow B., Abraham E.M., Aloui K., Atesoglu A., Attore F., Bassüllü Ç., Bey A., Garzuglia M., García-Montero L.G., Groot N., Guerin G., Laestadius L., Lowe A.J., Mamane B., Marchi G., Patterson P., Rezende M., Ricci S., Salcedo I., Diaz A.S.-P., Stolle F., Surappaeva V. and Castro R., The extent of forest in dryland biomes, *Science* **356**, 2017, 635–638, https://doi.org/10.1126/science.aam6527.

Blair J.B., Rabine D.L. and Hofton M.A., The Laser Vegetation Imaging Sensor (LVIS): ~~A~~a ~~M~~medium-~~A~~altitude, ~~D~~digitization-~~O~~only, ~~A~~airborne ~~L~~laser ~~A~~altimeter for ~~M~~mapping ~~V~~vegetation and ~~T~~topography, *ISPRS J. Photogramm. Remote Sens.* **54**, 1999, 115–122.

Bonan G.B. and Doney S.C., Climate, ecosystems, and planetary futures: ~~T~~the challenge to predict life in ~~E~~earth system models, *Science* 2018, 359.

Brando P.M., Goetz S.J., Baccini A., Nepstad D.C., Beck P.S.A. and Christman M.C., Seasonal and interannual variability of climate and vegetation indices across the Amazon, *Proc. Natl. Acad. Sci. U. S. A.* **107**, 2010, 14685–14690, https://doi.org/10.1073/pnas.0908741107.

Curtis P.G., Slay C.M., Harris N.L., Tyukavina A. and Hansen M.C., Classifying drivers of global forest loss, *Science* **361**, 2018, 1108 LP–1111.

DiMiceli C.M., Carroll M.L., Sohlberg R.A., Huang C., Hansen M.C. and Townshend J.R.G., Annual Global Automated MODIS Vegetation Continuous Fields (MOD44B) at 250 m Spatial Resolution for Data Years Beginning Day 65, 2000–2010, Collection 5 Percent Tree Cover, 2011.

Dubayah R., Goetz S.J., Blair J.B., Fatoyinbo T.E., Hansen M., Healey S.P., Hofton M.A., Hurtt G.C., Kellner J.R., Luthcke S.B. and Swatantran A., The global ecosystem dynamics investigation, In: *American Geophysical Union, Fall Meeting 2014,* 2014, AGU; San Francisco.

Fatoyinbo L., Pinto N., Hofton M., Simard M., Blair B., Saatchi S., Lou Y., Dubayah R., Hensley S., Armston J., Duncanson L. and Lavalle M., The 2016 NASA AfriSAR campaign: airborne SAR and Lidar measurements of tropical forest structure and biomass in support of future satellite missions, In: *2017 IEEE International Geoscience and Remote Sensing Symposium (IGARSS),* 2017, IEEE, 4286–4287, https://doi.org/10.1109/IGARSS.2017.8127949.

Fisher A., Scarth P., Armston J. and Danaher T., Relating foliage and crown projective cover in Australian tree stands, *Agric. For. Meteorol.* **259**, 2018, 39–47, https://doi.org/10.1016/j.agrformet.2018.04.016.

Friedl M.A., Sulla-Menashe D., Tan B., Schneider A., Ramankutty N., Sibley A. and Huang X.M., MODIS Collection 5 global land cover: algorithm refinements and characterization of new datasets, *Remote Sens. Environ.* **114**, 2010, 168–182, https://doi.org/10.1016/j.rse.2009.08.016.

Gerard F., Hooftman D., van Langevelde F., Veenendaal E., White S.M. and Lloyd J., MODIS VCF should not be used to detect discontinuities in tree cover due to binning bias. A comment on Hanan et al. (2014) and Staver and Hansen (2015), *Glob. Ecol. Biogeogr.* **26**, 2017, 854–859, https://doi.org/10.1111/geb.12592.

Goetz S. and Dubayah R., Advances in remote sensing technology and implications for measuring and monitoring forest carbon stocks and change, *Carbon Manag.* **2**, 2011, 231–244, https://doi.org/10.4155/cmt.11.18.

Goetz S.J., Hansen M., Houghton R.A., Walker W., Laporte N. and Busch J., Measurement and monitoring needs, capabilities and potential for addressing reduced emissions from deforestation and forest degradation under REDD, *Environ. Res. Lett.* **10**, 2015, (doi:Artn 12300110.1088/1748-9326/10/12/123001).

Hanan N.P., Tredennick A.T., Prihodko L., Bucini G. and Dohn J., Analysis of stable states in global savannas: is the CART pulling the horse?, *Glob. Ecol. Biogeogr.* **23**, 2014, 259–263, https://doi.org/10.1111/geb.12122.

Hansen M.C., DeFries R.S., Townshend J.R.G., Carroll M., Dimiceli C. and Sohlberg R.A., Global percent tree cover at a spatial resolution of 500 meters: first results of the MODIS vegetation continuous fields algorithm, *Earth Interact.* **7**, 2003, 1–15, https://doi.org/10.1175/1087-3562(2003)007<0001:GPTCAA>2.0.CO;2.

Hansen M.C., Stehman S. V.S.V., Potapov P. V.P.V., Loveland T.R., Townshend J.R.G., DeFries R.S., Pittman K.W., Arunarwati B., Stolle F., Steininger M.K., Carroll M. and DiMiceli C., Humid tropical forest clearing from 2000 to 2005 quantified by using multitemporal and multiresolution remotely sensed data, *Proc. Natl. Acad. Sci. U. S. A.* **105**, 2008, 9439–9444, https://doi.org/10.1073/pnas.0804042105.

Hansen M.C., Potapov P. V.P.V., Moore R., Hancher M., Turubanova S.A., Tyukavina A., Thau D., Stehman S. V.S.V., Goetz S.J., Loveland T.R., Kommareddy A., Egorov A., Chini L., Justice C.O. and Townshend J.R.G., High-resolution global maps of 21st-century forest cover change, *Science* **342**, 2013, 850–853, https://doi.org/10.1126/science.1244693.

Harding D.J., Lefsky M.A., Parker G.G. and Blair J.B., Laser altimeter canopy height profiles methods and validation for closed-canopy, broadleaf forests, *Remote Sens. Environ.* **76**, 2001, 283–297, https://doi.org/10.1016/S0034-4257(00)00210-8.

Hirota M., Holmgren M., Van Nes E.H. and Scheffer M., Global resilience of tropical forest and savanna to critical transitions, *Science* **334**, 2011, 232–235, https://doi.org/10.1126/science.1210657.

Hopkinson C. and Chasmer L., Testing LiDAR models of fractional cover across multiple forest ecozones, *Remote Sens. Environ.* **113**, 2009, 275–288, https://doi.org/10.1016/j.rse.2008.09.012.

Huete A., Didan K., Miura T., Rodriguez E.P., Gao X. and Ferreira L.G., Overview of the radiometric and biophysical performance of the MODIS vegetation indices, *Remote Sens. Environ.* **83**, 2002, 195–213, https://doi.org/10.1016/S0034-4257(02)00096-2.

Jennings S.B., Brown N.D. and Sheil D., Assessing forest canopies and understorey illumination: canopy closure, canopy cover and other measures, *Forestry* **72**, 1999, 59–73, https://doi.org/10.1093/forestry/72.1.59.

Korhonen L., Korpela I., Heiskanen J. and Maltamo M., Airborne discrete-return LIDAR data in the estimation of vertical canopy cover, angular canopy closure and leaf area index, *Remote Sens. Environ.* **115**, 2011, 1065–1080, https://doi.org/10.1016/j.rse.2010.12.011.

Lefsky M.A., A global forest canopy height map from the Mmoderate Rresolution Iimaging Sspectroradiometer and the Ggeoscience Llaser Aaltimeter Ssystem, *Geophys. Res. Lett.* **37**, 2010, https://doi.org/10.1029/2010GL043622.

Lefsky M.A., Cohen W.B., Parker G.G. and Harding D.J., Lidar Rremote Ssensing for Eecosystem Sstudies, *Bioscience* **52**, 2002, 19, https://doi.org/10.1641/0006-3568(2002)052[0019:LRSFES]2.0.CO;2.

Lewis S.L., Lloyd J., Sitch S., Mitchard E.T.A. and Laurance W.F., Changing Eecology of Ttropical Fforests: Eevidence and Ddrivers, *Annu. Rev. Ecol. Evol. Syst.* **40**, 2009, 529–549, https://doi.org/10.1146/annurev.ecolsys.39.110707.173345.

Lewis S.L., Edwards D.P. and Galbraith D., Increasing human dominance of tropical forests, *Science* **349**, 2015, 827–832, https://doi.org/10.1126/science.aaa9932.

Los S.O., Rosette J.A.B., Kljun N., North P.R.J., Chasmer L., Suárez J.C., Hopkinson C., Hill R.A., van Gorsel E., Mahoney C. and Berni J.A.J., Vegetation height and cover fraction between 60° S and 60° N from ICESat GLAS data, *Geosci. Model Dev.* **5**, 2012, 413–432, https://doi.org/10.5194/gmd-5-413-2012.

Malhi Y., Wood D., Baker T.R., Wright J., Phillips O.L., Cochrane T., Meir P., Chave J., Almeida S., Arroyo L., Higuchi N., Killeen T.J., Laurance S.G., Laurance W.F., Lewis S.L., Monteagudo A., Neill D.A., Vargas P.N., Pitman N.C.A., Quesada C.A., Salomão R., Silva J.N.M., Lezama A.T., Terborgh J., Martínez R.V. and Vinceti B., The regional variation of aboveground live biomass in old-growth Amazonian forests, *Glob. Chang. Biol.* **12**, 2006, 1107–1138, https://doi.org/10.1111/j.1365-2486.2006.01120.x.

Morsdorf F., Kotz B., Meier E., Itten K. and Allgower B., Estimation of LAI and fractional cover from small footprint airborne laser scanning data based on gap fraction, *Remote Sens. Environ.* **104**, 2006, 50–61, https://doi.org/10.1016/j.rse.2006.04.019.

Nelson R., Ranson K.J., Sun G., Kimes D.S., Kharuk V. and Montesano P., Estimating Siberian timber volume using MODIS and ICESat/GLAS, *Remote Sens. Environ.* **113**, 2009, 691–701, https://doi.org/10.1016/j.rse.2008.11.010.

Pan Y., Birdsey R.A., Fang J., Houghton R., Kauppi P.E., Kurz W.A., Phillips O.L., Shvidenko A., Lewis S.L., Canadell J.G., Ciais P., Jackson R.B., Pacala S.W., McGuire A.D., Piao S., Rautiainen A., Sitch S. and Hayes D., A Llarge and Ppersistent Ccarbon Ssink in the Wworld's Fforests, *Science* **333**, 2011, 988–993, https://doi.org/10.1126/science.1201609.

Phillips O.L., Aragão L.E.O.C., Lewis S.L., Fisher J.B., Lloyd J., López-González G., Malhi Y., Monteagudo A., Peacock J., Quesada C.A., Van Der Heijden G., Almeida S., Amaral I., Arroyo L., Aymard G., Baker T.R., Bánki O., Blanc L., Bona D., Brando P., Chave J., De Oliveira Á.C.A., Cardozo N.D., Czimczik C.I., Feldpausch T.R., Freitas M.A., Gloor E., Higuchi N., Jiménez E., Lloyd G., Meir P., Mendoza C., Morel A., Neill D.A., Nepstad D., Patiño S., Peñuela M.C., Prieto A., Ramírez F., Schwarz M., Silva J., Silveira M., Thomas A.S., Steege H. Ter, Stropp J., Vásquez R., Zelazowski P., Dávila E.A., Andelman S., Andrade A., Chao K.J., Erwin T., Di Fiore A., Honorio E.C., Keeling H., Killeen T.J., Laurance W.F., Cruz A.P., Pitman N.C.A., Vargas P.N., Ramírez-Angulo H., Rudas A., Salamão R., Silva N., Terborgh J. and Torres-Lezama A., Drought sensitivity of the amazon rainforest, *Science* **323**, 2009, 1344–1347, https://doi.org/10.1126/science.1164033.

Rautiainen M., Stenberg P. and Nilson T., Estimating canopy cover in Scots pine stands, *Silva Fenn.* **39**, 2005, 137–142, (doi:Artn 40210.14214/Sf.402).

Riano D., Chuvieco E., Salas J. and Aguado I., Assessment of different topographic corrections in Landsat-TM data for mapping vegetation types (2003), *IEEE Trans. Geosci. Remote Sens.* **41**, 2003, 1056–1061, https://doi.org/10.1109/Tgrs.2003.811693.

Saatchi S.S., Harris N.L., Brown S., Lefsky M., Mitchard E.T.A., Salas W., Zutta B.R., Buermann W., Lewis S.L., Hagen S., Petrova S., White L., Silman M. and Morel A., Benchmark map of forest carbon stocks in tropical regions across three continents, *Proc. Natl. Acad. Sci.* **108**, 2011, 9899–9904, https://doi.org/10.1073/pnas.1019576108.

Sexton J.O., Song X.-P., Feng M., Noojipady P., Anand A., Huang C., Kim D.-H., Collins K.M., Channan S., DiMiceli C. and Townshend J.R., Global, 30-m resolution continuous fields of tree cover: Landsat-based rescaling of MODIS vegetation continuous fields with lidar-based estimates of error, *Int. J. Digit. Earth* **6**, 2013, 427–448, https://doi.org/10.1080/17538947.2013.786146.

Sexton J.O., Noojipady P., Song X.-P., Feng M., Song D.-X., Kim D.-H., Anand A., Huang C., Channan S., Pimm S.L. and Townshend J.R., Conservation policy and the measurement of forests, *Nat. Clim. Chang.* **6**, 2016, 192–196.

Simard M., Pinto N., Fisher J.B. and Baccini A., Mapping forest canopy height globally with spaceborne lidar, *J. Geophys. Res.* **116**, 2011, https://doi.org/10.1029/2011JG001708.

Skole D. and Tucker C., Tropical Ddeforestation and Hhabitat Ffragmentation in the Amazon: Ssatellite Ddata from 1978 to 1988, *Science* **260**, 1993, 1905–1910, https://doi.org/10.1126/science.260.5116.1905.

Smith ~~M. N.~~M.N., Stark ~~S. C.~~S.C., Taylor ~~T. C.~~T.C., Ferreira ~~M. L.~~M.L., de Oliveira E., Restrepo-Coupe N., Chen S., Woodcock T., dos Santos ~~D. B.~~D.B., Alves ~~L. F.~~L.F., Figueira M., de Camargo ~~P. B.~~P.B., de Oliveira ~~R. C.~~R.C., Aragão ~~L. E.~~L.E., Falk ~~D. A.~~D.A., McMahon ~~S. M.~~S.M., Huxman ~~T. E.~~T.E. and Saleska ~~S. R.~~S.R., Seasonal and drought related changes in leaf area profiles depend on height and light environment in an Amazon forest, *New Phytol.* **222**, 2019 1284–1297, https://doi.org/10.1111/nph.15726.

Song C. and Woodcock C.E.E., Monitoring forest succession with multitemporal Landsat images: factors of uncertainty, *IEEE Trans. Geosci. Remote Sens.* **41**, 2003, 2557–2567, https://doi.org/10.1109/Tgrs.2003.818367.

Staver A.C. and Hansen M.C., Analysis of stable states in global savannas: ~~I~~is the CART pulling the horse? - a comment, *Glob. Ecol. Biogeogr.* 2015, https://doi.org/10.1111/geb.12285.

Staver A.C., Archibald S. and Levin S.A., The global extent and determinants of savanna and forest as alternative biome states, *Science* **334**, 2011, 230–232, https://doi.org/10.1126/science.1210465.

Tang H. and Dubayah R., Light-driven growth in Amazon evergreen forests explained by seasonal variations of vertical canopy structure, *Proc. Natl. Acad. Sci. U. S. A.* **114**, 2017, https://doi.org/10.1073/pnas.1616943114.

Tang H., Dubayah R., Swatantran A., Hofton M., Sheldon S., Clark D.B. and Blair B., Retrieval of vertical LAI profiles over tropical rain forests using waveform lidar at ~~l~~La ~~s~~Selva, ~~e~~Costa ~~r~~Rica, *Remote Sens. Environ.* **124**, 2012 https://doi.org/10.1016/j.rse.2012.05.005.

Tang H., Brolly M., Zhao F., Strahler A.H., Schaaf C.L., Ganguly S., Zhang G. and Dubayah R., Deriving and validating Leaf Area Index (LAI) at multiple spatial scales through lidar remote sensing: ~~A~~a case study in Sierra National Forest, CA, *Remote Sens. Environ.* **143**, 2014, https://doi.org/10.1016/j.rse.2013.12.007.

Tang H., Ganguly S., Zhang G., Hofton M.A., Nelson R.F. and Dubayah R., Characterizing leaf area index (LAI) and vertical foliage profile (VFP) over the United States, *Biogeosciences* **13**, 2016, 239–252, https://doi.org/10.5194/bg-13-239-2016.

Tang H., Song X.P., Zhao F., Strahler A., Schaaf C., Goetz S., Huang C., Hansen M. and Dubayah R., Definition and measurement of tree cover: ~~A~~a comparative analysis of field-, lidar- and Landsat-based tree cover estimations in the Sierra national forests, USA, ~~*Agricultural and Forest Meteorology*~~*Agric. For. Meteorol.* **268**, 2019, 258–268.

Townshend J.R., Masek J.G., Huang C.Q., Vermote E.F., Gao F., Channan S., Sexton J.O., Feng M., Narasimhan R., Kim D., Song K., Song D.X., Song X.P., Noojipady P., Tan B., Hansen M.C., Li M.X. and Wolfe R.E., Global characterization and monitoring of forest cover using Landsat data: opportunities and challenges, *Int. J. Digit. Earth* **5**, 2012, 373–397, https://doi.org/10.1080/17538947.2012.713190.

Watson J.E.M., Evans T., Venter O., Williams B., Tulloch A., Stewart C., Thompson I., Ray J.C., Murray K., Salazar A., McAlpine C., Potapov P., Walston J., Robinson J.G., Painter M., Wilkie D., Filardi C., Laurance W.F., Houghton R.A., Maxwell S., Grantham H., Samper C., Wang S., Laestadius L., Runting R.K., Silva-Chávez G.A., Ervin J. and Lindenmayer D., The exceptional value of intact forest ecosystems, *Nat. Ecol. Evol.* 2018, https://doi.org/10.1038/s41559-018-0490-x.

Wright S.J., Kitajima K., Kraft N.J.B., Reich P.B., Wright I.J., Bunker D.E., Condit R., Dalling J.W., Davies S.J., Díaz S., Engelbrecht B.M.J., Harms K.E., Hubbell S.P., Marks C.O., Ruiz-Jaen M.C., Salvador C.M. and Zanne A.E., Functional traits and the growth-mortality trade-off in tropical trees, *Ecology* **91**, 2010, 3664–3674, https://doi.org/10.1890/09-2335.1.

Yuan H., Dickinson R.E., Dai Y., Shaikh M.J., Zhou L., Shangguan W. and Ji D., A 3D canopy radiative transfer model for global climate modeling: ~~Đ~~description, validation, and application, *J. Clim.* **27**, 2014, 1168–1192, https://doi.org/10.1175/JCLI-D-13-00155.1.

~~Appendix A.~~Appendix A. Supplementary data

Multimedia Component 1

Supplementary material

alt-text: Image 1

Highlights

- First global canopy cover data set from a lidar satellite

- High sensitivity of lidar-based canopy cover to dense forests
- A quality-driven product complement to area-focused forest cover mapping

---

Queries and Answers

Query:

Your article is registered as a regular item and is being processed for inclusion in a regular issue of the journal. If this is NOT correct and your article belongs to a Special Issue/Collection please contact m.venkatesan@elsevier.com immediately prior to returning your corrections.

Answer: This article is a regular submission.

Query:

Please confirm that given names and surnames have been identified correctly and are presented in the desired order, and please carefully verify the spelling of all authors' names.

Answer: The names and surnames are correct and presented in the desired order.

Query:

The author names have been tagged as given names and surnames (surnames are highlighted in teal color). Please confirm if they have been identified correctly.

Answer: They all are correct.

Query:

The country name "United States" has been inserted for the correspondence field. Please check and confirm if correct.

Answer: Correct.

Query:

Fig. 8 is not cited in the text. Please check if the suggested citation is in the appropriate place, and correct if necessary.

Answer: Necessary changes have been made in the same paragraph.

Query:

Have we correctly interpreted the following funding source(s) and country names you cited in your article: "NASA".

Answer: The last NASA Grant NNX16AP74G does not seem to have a link. All others are correct.

Query:

Supplementary caption was not provided. Please check the suggested data if appropriate, and correct if necessary.

Answer: The supplementary data contains captions (in bold) for figures (Fig. S1 and Fig. S2) and table (Table S1).
Attachments: mmc1.docx